NOVEMBER 1979 PPPL-1600
UC-20g

FLUCTUATIONS AND TRANSPORT IN AN INHOMOGENEOUS PLASMA

BY

W. M. NEVINS AND L. CHEN

PLASMA PHYSICS LABORATORY

PRINCETON UNIVERSITY

Fluctuations and Transport in an Inhomogeneous Plasma

William M. Nevins* and Liu Chen

Plasma Physics Laboratory, Princeton Univc ity

Princeton, New Jersey 08544

A formalism is developed for calculating the equilibrium fluctuation level in an inhomogeneous lasma. This formalism is applied to the collisionless drift wave in a sheared magnetic field. The fluctuation level is found to be anomalously large due to both the presence of weakly damped normal modes and convective amplification. As the magnetic shear is reduced, the steady-state fluctuation spectrum is found to increase both in coherence and in amplitude. The transport associated with this mode is evaluated. The diffusion coefficient is found to scale as $D \propto B^2/nT^{1/2}$.

* New address: Lawrence Livermore Laboratory, M-Division, L-439, P.O. Box 808, Livermore, CA 94550

I. INTRODUCTION.

Any calculation of the anomalous transport caused by micro-instabilities in magnetized plasmas requires an evaluation of the equilibrium fluctuation level associated with these modes. Much of the previous work in this field has dealt with nonlinear effects that might limit the amplitude of the linearly unstable normal modes, leading to a steady-state fluctuation level.[1]

Recent works[2-7] have demonstrated that, in a slab geometry with weak inhomogenity (i.e., $\rho_s/L_n \ll 1$), the collisionless drift mode is stabilized by the presence of magnetic shear. This demonstration presents us with a unique possibility to calculate both the fluctuation spectrum, and the transport coefficients within the context of linear theory since the fluctuation spectrum may be calculated by balancing the Cherenkov emission from discrete particles against the linear damping rate of the radial eigenmodes.

Although the collisionless drift mode is found to be linearly stable when the full radial mode structure is taken into account, it remains locally unstable, and, hence, one may expect that convective amplification will lead to anomalously high fluctuation levels. Since the normal modes are known to be stable, the fluctuation spectrum may be calculated by the method of shielded test particles.[8] Kent and Taylor[9] have used this method to study the fluctuation level due to convective amplification in the absence of normal modes (see also Baldwin and Callen[10]).

Here, we generalize their work to include the contribution of weakly damped normal modes to the fluctuation spectrum. An important result of this work is the formalism, developed in Sec. II, in which the contribution of each normal mode to the equilibrium fluctuation spectrum is expressed in terms of the eigenfrequency, an additional parameter that characterizes the coupling strength of the mode, and the eigenfunction; together with various parameters that characterize the equilibrium plasma.

M. True[11] has also studied the fluctuation level of normal modes in an inhomogeneous plasma, but his formalism is limited to situations in which the governing linear eigenmode equation has the form of the Weber equation. We allow for more general second-order differential equations in developing our formalism in Sec. II, and in Sec. III we show how the various factors appearing in our expression for the spectral density may be evaluated by using phase integral (i.e., WKB) methods. In Sec. IV we focus on the fluctuation level of the collisionless drift mode, and show that, as the magnetic shear becomes progressively weaker, the fluctuations in these modes increase dramatically. In Sec. V we evaluate the anomalous transport associated with the collisionless drift mode in a plasma slab, and in Sec. VI we comment on the limits of validity of this calculation.

II. THE SPECTRAL DENSITY.

The fluctuation spectrum of an inhomogeneous, but linearly stable plasma may be calculated by superimposing the shielding clouds of statistically independent test particles.[8-10] We consider a plane slab model with x used to label the non-ignorable coordinate. The equilibrium plasma is assumed to depend only on x, so we make use of a Fourier transform representation in the two ignorable coordinates, y and z. The electrostatic potential may then be written as

$$\phi_{\underline{k}}(x,t) = \int_{-\infty}^{\infty} \frac{d\omega}{2\pi} \tilde{\phi}_{\underline{k}}(x,\omega)\exp(-i\omega t) \quad , \tag{1}$$

where $\underline{k} = k_y\hat{y} + k_z\hat{z}$ lies in the y-z plane. In a linearly stable plasma the integration contour may be taken along the real ω axis. We make this choice of integration path, so hereafter ω is taken to be real. In addition, the $\underline{k}$ dependence of $\tilde{\phi}_{\underline{k}}(x,\omega)$ is suppressed.

The electrostatic response of the plasma is described by Poisson's equation. In many cases of interest, Poisson's equation takes the form

$$P(x,\omega)\tilde{\phi}'' + R(x,\omega)\tilde{\phi} = 4\pi\tilde{\rho} \quad , \tag{2}$$

where primes denote derivatives with respect to x, and $\tilde{\rho}(x,\omega)$ is the (Fourier transformed in y, z, and t) external charge density.

Equation (2) may be formally solved by the use of a Green's function,[12] yielding

$$\tilde{\phi}(x,\omega) = \int_{-\infty}^{\infty} dx' g(x,x',\omega)\tilde{\rho}(x',\omega) \quad . \tag{3}$$

The propagator, g , is given by

$$g(x,x',\omega) = \frac{4\pi}{W(\omega)P(x',\omega)}[\phi_+(x,\omega)\phi_-(x',\omega)h(x-x') + \phi_+(x',\omega)\phi_-(x,\omega)h(x'-x)] \tag{4}$$

where $\phi_+(x,\omega)$ and $\phi_-(x,\omega)$ are the solutions to the homogeneous equation

$$\phi'' + Q(x,\omega)\phi = 0 \tag{5}$$

with

$$Q(x,\omega) \equiv R(x,\omega)/P(x,\omega) \quad . \tag{6}$$

The solutions, ϕ_+ and ϕ_- are constructed to satisfy the appropriate boundry conditions at + and - infinity respectively. $W(\omega)$ is the Wronskian of these two solutions, which may be shown to be independent of x,[12]

$$W(\omega) = \phi_-(x,\omega)\phi_+'(x,\omega) - \phi_-'(x,\omega)\phi_+(x,\omega) \quad , \tag{7}$$

and $h(x)$ is the Heaviside function,

$$h(x) = \begin{cases} 0 & \text{for } x < 0 \\ 1 & \text{for } x > 0 \end{cases} \quad . \tag{8}$$

The charge density of a test particle with phase variables $\underline{R}(t)$, $\underline{V}(t)$ is given by

$$\tilde{\rho}(x', \omega | \underline{R}, \underline{V}) = q \int_{-\infty}^{\infty} dt' \exp i[\omega t' - \underline{k} \cdot \underline{R}(t')] \delta[x' - X(t')] \quad , \tag{9}$$

where X is the x component of $\underline{R}$. A considerable simplification is achieved by ignoring finite Larmor radius effects in evaluating $\tilde{\rho}$. This approximation is sufficient for evaluating the fluctuation level of collisionless drift modes when $T_e > T_i$ as the wave length of the dominant modes are found to be large in comparison to both the electron and ion gyroradii. We adopt it here, and obtain

$$\tilde{\rho}(x, \omega | X, V_{||}) = 2\pi q \delta[\omega - k_{||}(X) V_{||}] \delta(x' - X) \quad . \tag{10}$$

The interested reader will find a treatment of finite Larmor radius corrections to $\tilde{\rho}$ in Ref. 9.

The shielding cloud of an isolated test particle is obtained by substituting Eq. (10) into Eq. (3). The two time, two point correlation function is obtained by superimposing the shielding clouds of the statistically independent test particles, yielding

$$\langle \phi(x',t+\tau)\phi^*(x,t)\rangle = \sum_s q_s^2 \int dV_{||}\, dX\, F_s(V_{||},X) \int d\omega d\omega' \exp\{-i[(\omega'-\omega)t + \omega'\tau]\}$$

$$\times \delta[\omega - k_{||}(X)V_{||}]\,\delta[\omega' - k_{||}(X)V_{||}]\, g(x',X,\omega')\, g^*(x,X,\omega) \quad , \tag{11}$$

where $F_s(V_{||},X)$ is the distribution function of species s. Substituting Eq. (4) for g, and using the delta functions to perform two integrations, we obtain

$$C(x,x',\tau) \equiv \frac{q_e^2}{T_e^2} \langle \phi(x',t+\tau)\,\phi^*(x,t)\rangle$$

$$= \int_{-\infty}^{\infty} \frac{d\omega}{2\pi}\, S(x,x',\omega) \quad , \tag{12}$$

where the cross-spectrum is given by

$$S(x,x',\omega) = \sum_s \frac{32\pi^4 q_e^2 q_s^2}{T_e^2 |W(\omega)|^2} \left\{ \phi_+(x,\omega)\phi_+^*(x',\omega) \int_{-\infty}^{\min(x,x')} \frac{dX}{k_{||}(X)|P(X,\omega)|^2} \right.$$

$$\times F_s(\omega/k_{||},X)|\phi_-(X,\omega)|^2 + \phi_+(x,\omega)\phi_-^*(x',\omega)h(x-x')$$

$$\times \int_{x'}^{x} \frac{dX}{k_{||}|P|^2} F_s(\omega/k_{||},X)\phi_+^*(X,\omega)\phi_-(X,\omega) + \phi_-(x,\omega)\phi_+^*(x',\omega)h(x'-x)$$

$$\times \int_{x}^{x'} \frac{dX}{k_{||}|P|^2} F_s(\omega/k_{||},X)\phi_+(X,\omega)\phi_-^*(X,\omega) + \phi_-(x,\omega)\phi_-^*(x',\omega)$$

$$\left. \times \int_{\max(x,x')}^{\infty} \frac{dX}{k_{||}|P|^2} F_s(\omega/k_{||},X)|\phi_+(X,\omega)|^2 \right\} \quad . \tag{13}$$

We now assume that the cross-spectrum is dominated by weakly damped normal modes. In the neighborhood of the ℓ^{th} normal mode we may approximate the Wronskian by

$$|W(\omega)|^2 \simeq \left|\frac{dW}{d\omega_\ell}\right|^2 [(\omega-\Omega_\ell)^2 + \gamma_\ell^2] \quad , \tag{14}$$

where Ω_ℓ and γ_ℓ are the real and imaginary parts of the eigenfrequency, ω_ℓ . Retaining just the contributions to the cross-spectrum from frequencies in the neighborhood of these eigenfrequencies, we obtain

$$S(x,x',\omega) \simeq \sum_\ell S_\ell(x,x')R(\omega-\Omega_\ell,\gamma_\ell) \quad , \tag{15}$$

where

$$S_\ell(x,x') = \frac{32\pi^4 q_e^2 q_s^2 \tau_\ell}{|dW/d\omega_\ell|^2 T_e^2} \int_{-\infty}^{\infty} \frac{dX}{k_{||}|P|^2} F_s(\Omega_\ell/k_{||},X)|\phi_\ell(x)|^2 \phi_\ell(x)\phi_\ell^*(x') \quad , \tag{16}$$

$\phi_\ell(x)$ is the eigenfunction of the ℓ^{th} normal mode, τ_ℓ is the decay time, $-1/\gamma_\ell$, and

$$R(\Omega,\gamma) \equiv \frac{1}{\pi} \frac{\gamma}{\Omega^2 + \gamma^2} \quad . \tag{17}$$

Note that

$$\lim_{\gamma \to 0} R(\Omega,\gamma) = \delta(\Omega) \quad .$$

Similarly, we may write the contribution of each weakly damped normal mode to the cross-correlation function as

$$C_\ell(x,x',\tau) = \sum_s \frac{16\pi^3 q_e^2 q_s^2}{|dW/d\omega_\ell|^2 T_e^2 |\gamma_\ell|} \phi_\ell(x)\phi_\ell^*(x') \times \left(\int_{-\infty}^{\infty} \frac{dX}{k_{||}|P|^2} F_s(\Omega_\ell/k_{||},X)|\phi_\ell(X)|^2 \right) e^{-i\omega_\ell \tau} \quad , \tag{18}$$

so that

$$C(x,x',\tau) = \sum_\ell C_\ell(x,x',\tau) \quad . \tag{19}$$

The numerator in Eq. (18), which is proportional to the number of particles resonant with the ℓ^{th} normal mode, describes the spontaneous (Cherenkov) emission by discrete particles into the ℓ^{th} mode, while the denominator includes the linear damping rate. Hence, Eq. (18) may be interpreted as describing a balance between the power input to the ℓ^{th} mode from Cherenkov emission and the power lost due to the linear damping of the normal mode.

Finally, we note that in calculating the contribution of weakly damped modes to the fluctuation spectrum, each mode need only be characterized by the *complex frequency*, ω_ℓ, the *mode structure*, $\phi_\ell(x)$, and one additional parameter, $|dW/d\omega_\ell|$.

III. THE WRONSKIAN

In order to proceed with our analysis of the fluctuation spectrum, we must calculate the Wronskian of the solutions to Eq. (5), $\phi_+(x,\omega)$ and $\phi_-(x,\omega)$, in the neighborhood of the normal mode frequencies. Asymptotic approximations to these solutions may be constructed through the WKB approximation. This is accomplished by analytically continuing the function $Q(x,\omega)$ into the complex x plane and examining the Stokes structure.[13] Figure 1 illustrates a Stokes structure characteristic of a convectively unstable plasma. Here, $\phi_+(x,\omega)$ is the solution to Eq. (5) that is subdominant in region I, to the right of the turning point labeled V_+, while $\phi_-(x,\omega)$ is subdominant in region V to the left of turning point V_-, i.e.,

$$\phi_+(x,\omega) = (x,V_+)_s = \frac{A^{-1/2}}{Q^{1/4}} \exp i\left\{ \int_{V_+}^{x} Q^{1/2}\, dx \right\} \quad \text{(region I)} \ , \tag{20}$$

and

$$\phi_-(x,\omega) = (V_-,x)_s = \frac{A^{-1/2}}{Q^{1/4}} \exp i\left\{ \int_{V_-}^{x} Q^{1/2}\, dx \right\} \quad \text{(region V)} \ , \tag{21}$$

where A is an arbitrary function of ω that will be employed later in normalizing these solutions, and the notation $(x,V_+)_s$, $(V_-,x)_s$ is adapted from Heading.[13]

With the aid of the WKB connection formulae, these solutions may both be continued into region III, where

$$\phi_+(x,\omega) = (x,V_+)_d + i(V_+,x)_s \quad \text{(region III)} \ , \tag{22}$$

and

$$\phi_-(x,\omega) = [V_-,V_+](V_+,x)_s + i[V_+,V_-](x,V_+)_d \quad \text{(region III)} \ . \tag{23}$$

The Wronskian is then given by

$$W(\omega) = \frac{2i}{A} \cos I(\omega) \ , \tag{24}$$

where

$$I(\omega) \equiv \int_{V_-}^{V_+} Q^{1/2}\, dx \ , \tag{25}$$

and A will be identified as the amplification factor.[9]

The normal mode frequencies are determined by requiring that the Wronskian vanish. This reproduces the usual WKB resonance condition,

$$I(\omega_\ell) = (\ell + 1/2)\pi \ . \tag{26}$$

Hence, at a normal mode frequency $dW/d\omega_\ell$ is given by

$$\left|\frac{dW}{d\omega_\ell}\right| = |T_\ell|/A_\ell \quad , \tag{27}$$

where

$$T_\ell \quad 2\frac{dI}{d\omega_\ell} = \int_{V_-}^{V_+} Q^{-1/2}\,\frac{\partial Q}{\partial \omega}\,dx \tag{28}$$

may be evaluated for each normal mode by performing the indicated integration.

We note that, within the WKB approximation, Q is simply k_x. Since the group velocity is given by $V_g = (\partial k_x/\partial\omega)^{-1}$, T_ℓ may be written as

$$T_\ell = 2\int_{V_-}^{V_+} \frac{dx}{V_g} \quad , \tag{29}$$

and hence, T_ℓ may be interpreted as the time for a signal to propagate from one turning point to the other and back at the group velocity, i.e., T_ℓ is the period of oscillation of phonons trapped in the "potential well", $-Q(x,\omega)$.

It is convenient to choose ϕ_ℓ such that

$$\int_{-\infty}^{\infty} dx\,|\phi_\ell(x)|^2 = 1 \quad , \tag{30}$$

where the integral is taken along the real x axis. Figure 2 shows the Stokes structure at a normal mode frequency. We note that along the real axis between 0 and $0'$ the eigenfunction is well approximated by

$$\phi_\ell(x) \simeq \frac{A_\ell^{-1/2}}{Q^{1/4}}\exp i\int_0^x Q^{1/2}\,dx \quad . \tag{31}$$

When the Stokes structure resembles Fig. 2, there exists a point x_ℓ' on $(\mathcal{O},\mathcal{O}')$ such that $\mathrm{Im}\, Q^{1/2}(x_\ell', \omega_\ell) = 0$. The eigenfunction $\phi_\ell(x)$ has a maximum at this point. In the neighborhood of this point, it may be approximated by a Gaussian centered at x_ℓ' with a width

$$\Delta x_\ell' = \left(\frac{k_\ell'}{\mathrm{Im}\, \partial Q / \partial x_\ell'} \right)^{1/2} \tag{32}$$

where $k_\ell' = Q^{1/2}(x', \omega_\ell)$. Hence,

$$\phi_\ell(x) \sim \frac{1}{A_\ell k_\ell'} \exp 2\left(\int_0^{x_\ell'} \mathrm{Im}\, Q^{1/2}(x, \omega_\ell)\, dx - (x - x_\ell')^2 / \Delta x_\ell'^2 \right) \tag{33}$$

in the neighborhood of x_ℓ', where the branch of $Q^{1/2}$ is chosen such that $\Delta x_\ell'^2$ is greater than zero.

When the convective instability is strong, the turning points will be far from the real axis, and most of the contribution to $\int |\phi_\ell(x)|^2 dx$ comes from the region about x_ℓ', as well as the analogous region centered about x_ℓ'' on $(\mathcal{O},\mathcal{O}'')$, where $\mathrm{Im}\, Q^{1/2}(x_\ell'', \omega_\ell)$ again vanishes. Hence, our normalization condition yields

$$A_\ell = (\pi/2)^{1/2} k_\ell'^{-1} \Delta x_\ell' \exp\left(2 \int_0^{x_\ell'} \mathrm{Im}\, Q^{1/2}(x, \omega_\ell)\, dx \right) + (\text{terms with } x_\ell' \to x_\ell'') \ . \tag{34}$$

This expression is reminicent of the convective amplification factor of Kent and Taylor.[9] In recent work on the collisionless drift mode[6,14] an amplification factor, written as $e^{\pi a}$ has been derived by considering the scattering of a signal as it passes through the locally unstable region about the rational surface.

In order of magnitude, these amplification factors are related by $(k_\ell \Lambda_\ell / \Gamma_\ell)(\quad/T_\ell) \quad e^{\pi a}$.

The contribution of the ℓ^{th} normal mode to the spectral density, Eq. (16), may be written in the form

$$S_\ell(x,x') = \sum_s \frac{32\pi^4 q_e^2 q_s^2}{T_e^2} \frac{\gamma_\ell \Lambda_\ell^2}{|T_\ell|^2} \left\{ \int_{-\infty}^{\infty} \frac{dx}{k_\parallel |p|} F_s(\omega_\ell/k_\parallel, x) |\phi_\ell(x)|^2 \right\} \phi_\ell(x) \phi_\ell^*(x') , \tag{35}$$

where $T_\ell, \Lambda_\ell, \gamma_\ell$ and $\phi_\ell(x)$ may all be expressed in terms of phase integrals. This fluctuation level will become anomalously large if Λ_ℓ and/or γ_ℓ become very large. In Sec. IV, we apply this formalism to the collisionless drift mode in a sheared magnetic field, and find that the fluctuation level is indeed substantial when the magnetic shear is weak.

IV. FLUCTUATION SPECTRUM OF THE COLLISIONLESS DRIFT MODE

A well-known example of a plasma wave that is convectively unstable when all of the normal modes are known to be damped is the collisionless drift wave in a plasma slab with a sheared magnetic field (provided that the equilibrium variations are sufficiently weak and $\nabla T_i = 0$). This mode is described by an equation of the form of Eq. (5) with Q given by[15]

$$Q(\tilde{x},\Omega) = T_e/T_i - b + \frac{(1+T_e/T_i)\Omega + (\Omega-1)\xi_e Z(\xi_e)}{(T_i/T_e+\Omega)\xi_i Z(\xi_i)} , \tag{36}$$

where $\tilde{x}$ is the distance from the rational surface, $\tilde{x} = [x - x_r(\underline{k})]/\rho_s$, while $\Omega = \omega/\omega^*$, with $\rho_s = (m_i T_e)^{1/2}/eB$, and $\omega^* = (-k_\perp T_e/eB)(1/L_n)$. In addition, $\xi_e = 2^{-1/2}(m_e/m_i)^{1/2}(L_s/L_n)(\Omega/\tilde{x})$, $\xi_i = 2^{-1/2}(T_e/T_i)^{1/2}(L_s/L_n)(\Omega/\tilde{x})$, and $b = (k_\perp \rho_s)^2$; T_e, T_i and m_e, m_i are the electron and ion temperature

and mass respectively. $Z(\cdot)$ is the plasma dispersion function, L_s is the magnetic shear length, L_n is the density gradient scale length, and $k_\perp$ is the component of $\underline{k}$ perpendicular to $\underline{B}$ (but recall that $\underline{k}$ as defined here lies in the y-z plane).

Previous work has demonstrated that the radial eigenmodes of the collisionless drift wave can be obtained through the WKB approximation.[4] In addition, it has been determined that, while this mode is always damped in the presence of magnetic shear,[5-7] the damping rate becomes exponentially small in (L_s/L_n) when this parameter is greater than a critical value, $(L_s/L_n)_c$, given approximately by[4]

$$(L_s/L_n)_c \simeq 3(m_i/m_e)^{1/4} \quad . \tag{37}$$

This fact, together with Eq. (35) suggests that the equilibrium fluctuation level in this mode will become very large in the limit of weak magnetic shear, $(L_s/L_n) > (L_s/L_n)_c$.

A. Decay Time

In order to obtain the decay time in this weak shear limit, one must take account of both the electron turning points, $\pm E$ and the ion sound turning points, $\pm P$, where we use the notation of Ref. 4. The Stokes structure characteristic of this weak magnetic shear limit is sketched in Fig. 3. This diagram differs somewhat from that shown in Ref. 4 because we have allowed for finite ion temperatures, and hence, Fig. 3 includes new physics — namely, ion Landau damping. It is evident from Fig. 3 that a radially localized solution must be subdominant in regions I and X of the complex x plane. The subdominant solutions in these regions may be continued into regions V and VI to obtain both the Wronskian and the dispersion

relation. The continuation of these solutions from regions I and X to regions V and VI is analogous to the problem of tunneling through an overdense potential barrier, which has been treated by Heading.[13] The resulting dispersion relation is most usefully expressed by expanding in the tunneling factor,

$$\delta = \exp 2i \int_{p}^{E} Q^{1/2} dx \tag{38}$$

where the branch of the square root is chosen such that $\mathrm{Im}\, Q^{1/2} > 0$. At lowest order, we obtain

$$I[\omega_\ell^{(0)}] = (\ell + 1/2)\pi \tag{39}$$

where $I(\omega)$ is given by Eq. (26), with the phase integral taken between the two electron turning points, $\pm E$, along a path that passes through $x = 0$. Similarly, $|dW/d\omega_\ell|$ is given by Eqs. (27) - (29) in the lowest order.

It was shown in Ref. 4 that the lowest order frequency must be real for $(L_s/L_n) > (L_s/L_n)_c$. Hence, the decay time $\tau_\ell = -1/\gamma_\ell$ is determined at first order in this expansion. We find[16]

$$\tau_\ell = T_\ell/\delta \quad . \tag{40}$$

In order to limit the dimensions of the parameter space in our numerical calculations, we fix the temperature at a value typical of Ohmically heated plasmas, $T_e/T_i = 4$, and take the mass ratio to be $m_e/m_i = 1/1837$. The factors characterizing the fluctuation spectrum are then functions of the single parameter, L_s/L_n. The various integrals involved have been evaluated numerically with R. White's WKB code.[17]

Figure 4 shows the decay time of modes $\ell = 0$ through $\ell = 2$ plotted against L_s/L_n. It is evident from this figure that the decay time of the collisionless drift modes can be made arbitrarily large by increasing L_s/L_n. In addition, the decay time of the $\ell = 0$ mode is much longer than the decay time of the other modes. Since the fluctuation level is proportional to τ_ℓ, the fluctuation level of the $\ell = 0$ modes greatly exceeds that of modes with $\ell \neq 0$. We will, therefore, ignore the fluctuations of modes with $\ell \neq 0$.

Figure 5 shows the decay time of the $\ell = 0$ mode plotted against b. The decay time is found to be strongly peaked. The existence of a most weakly damped mode at a value of b where the differential formulation of the radial eigenmode problem may reasonably be expected to be valid is signficant because it allows us to calculate the absolute fluctuation level within the differential formulation without any arbitrary cut-offs in b due to the breakdown of the differential formulation. In addition, the calculation of the fluctuation level is greatly simplified because we need only consider the fluctuation level of those modes in the neighborhood of this most weakly damped mode.

B. The Fluctuation Spectrum

The weakly damped modes are localized in a region where $\xi_i >> 1 >> \xi_e$. Hence, the contribution of Cherenkov emission from ions, which is proportional to $\exp(-\xi_i^2)$, may be ignored in comparison to the emission from electrons. The large value of ξ_i also allows us to approximate the function $P(\tilde{x},\Omega)$ of Eq. (2) by[15]

$$P(\tilde{x},\Omega) \sim \frac{\omega_{pi}^2}{\omega_{ci}^2} \frac{\Omega+T_i/T_e}{\Omega} \quad . \tag{41}$$

It follows from the small value of ϵ_e that F_e is nearly constant in the region of localization of the mode. Hence, the spectral density of the collisionless drift mode may be approximated by

$$S(x,x',\Omega) = \frac{4\pi^{1/2}}{n\rho_s^2 L_n}(L_s/\rho_s)g(b)\,|\phi_o(\tilde{x})|^2 R[\Omega-\Omega_o(b),\gamma_o(b)]$$

$$\cdot \exp[ik_o(\tilde{x}-\tilde{x}) - (\tilde{x}-\tilde{x}')^2/\Delta x_o^2 + 2(\tilde{x}-\tilde{x}')(\tilde{x}-\tilde{x}_o)/\Delta x_o^2]$$

$$+ \text{(terms with } \tilde{x}_o \to -\tilde{x}_o;\ k_o \to -k_o), \tag{42}$$

where we have assumed that $|\tilde{x}-\tilde{x}'| \ll \tilde{x}_o$, and $g(b)$ is given by

$$g(b) = \frac{\pi}{2^{3/2}}(m_e/m_i)^{1/2} \frac{\tau_o A_o^2}{\tilde{x}_o T_o^2} \frac{\Omega_o^2}{(\Omega_o+T_i/T_e)^2} \quad . \tag{43}$$

Figure 6 shows $g(b)$ at $L_s/L_n = 100$. Since it is sharply peaked, we choose to characterize it by an amplitude, g_o, a mean b_{max}, and a width Δb which may be determined as functions of L_s/L_n by fitting the numerically obtained values of $g(b)$ to the Gaussian,

$$g(b) \approx \frac{g_o}{\Delta b} \exp -[(b-b_{max})^2/\Delta b^2] \quad . \tag{44}$$

Using Eq. (44) to model $g(b)$ it is then a simple matter to integrate over ω and $\underline{k}$ to obtain the correlation function

$$C(s,\tau) = \tfrac{1}{2}\langle(e\phi/T_e)^2\rangle \{\exp[-i(\omega_m\tau + k_x s) - (s - V_g\tau)^2/2\Delta s^2] + \exp[-i(\omega_m\tau - k_x s) - (s + V_g\tau)^2/2\Delta s^2]\}\exp(-s^2/2\Delta x_m^2) , \quad (45)$$

where $s \equiv (x-x')/\rho_s$, $\tau \equiv (t-t')$, $\omega_m = \omega(b_{max})$, $k_x = Q^{1/2}[\omega_m, x_o(b_{max})]$, $\Delta s^2 = 2/(\partial k_x/\partial b_{max})^2 \Delta b^2$, $V_g = (\partial\omega_m/\partial b_{max})/(\partial k_x/\partial b_{max})$, and

$$\langle(e\phi/T_e)^2\rangle = \frac{g_o}{n\rho_s^2 L_n} . \quad (46)$$

Numerical values of the mean frequency ω_m and the correlation time, $\tau_c = 2^{1/2}\Delta s/V_g$ are shown in Fig. 7. ω_m is only very weakly dependent on L_s/L_n, while the correlation time is found to increase with L_s/L_n. Figures 8 - 11 show V_g, Δs, $k_x\rho_s$, $k_\perp\rho_s = b_{max}^{1/2}$ and $k_\parallel L_n$ as functions of L_s/L_n. Figure 9 also shows the correlation length in the inhomogeneous direction ℓ_x vs. L_s/L_n. The correlation length associated with phase mixing among normal modes, Δs, is found numerically to be large compared to $\Delta x_m = \Delta x_o(b_{max})$. Hence, $\ell_x \simeq 2^{1/2}\Delta x_m$.

The mean wave numbers and correlation lengths in the directions parallel and perpendicular to the magnetic field may be inferred from our expressions for the spectral density, Eq. (42). We find that $k_\parallel$, $k_\perp$ are nearly independent of L_s/L_n and are given by $k_\parallel L_n \simeq 0.11$, $k_\perp\rho_s \simeq 0.87$, for $50 < L_s/L_n < 100$, while the correlation lengths, $\ell_\parallel$ and $\ell_\perp$ increase with L_s/L_n (see Figs. 10 and 11). Hence, the wave-vectors are nearly perpendicular to the local magnetic field with $k_x \simeq k_\perp >> k_\parallel$.

Perhaps, the most interesting feature of the fluctuation spectrum is the large value of $\langle(e\phi/T_e)^2\rangle$ that may be achieved as L_s/L_n is increased. This is illustrated by Fig. 12. We find that the

numerically determined values of $\langle (e\phi/T_e)^2 \rangle$ are well fit to two significant figures by

$$\langle (e\phi/T_e)^2 \rangle \approx \frac{5 \times 10^{-2}}{n\rho_s^2 L_n} \exp\left[2\left[(L_s/L_n)/(L_s/L_n)_c\right]^{1/3}\right] , \tag{47}$$

where $(L_s/L_n)_c$ is given by Eq. (37). As a particular example, $\langle (e\phi/T_e)^2 \rangle$ is evaluated for a PLT-like plasma with $n = 10^{14}\ cm^{-3}$, $B = 10$ kG, and $T_e = 1$ keV. The result is shown by the scale on the right-hand side of Fig. 12.

It is evident from Fig. 12 that the fluctuation level of the collisionless drift modes becomes very large at moderate values of L_s/L_n. For the reference parameters $L_n = 10$ cm, $n = 10^{14}\ cm^{-3}$, $B = 10$ kG, and $T_e = 1$ keV, the fluctuations reach the level $\langle (e\phi/T_e)^2 \rangle^{1/2} \sim 10^{-2}$ at $L_s/L_n = 90$. Both the spatial amplification ($A_o^2 \sim 10^6$) and the long decay times ($\tau_o \sim 10^6 L_n/c_s$) contribute to this result.

We summarize the results of this section by noting that the fluctuation spectrum becomes more coherent, and the fluctuation amplitude increases dramatically as L_s/L_n is increased.

V. TRANSPORT

Having evaluated the steady state fluctuation spectrum in Sec. IV, we are now able to evaluate the transport associated with these fluctuations. The large fluctuation levels that are obtained in the limit of weak magnetic shear lead us to expect the transport rates will be anomalously large in this limit as well.

The transport driven by the equilibrium fluctuation spectrum of the collisionless drift waves may be expressed as an integral over the wave spectrum by assuming a linear response of the plasma to

the waves, and taking the appropriate moments of the drift kinetic equation.[18] In the absence of a temperature gradient, the electron particle and energy flux may be written as

$$\Gamma_e = -(\pi/2)^{1/2}\left[\left(\frac{T}{eB}\right)^2 \int dk_\perp \left(\frac{e\phi}{T}\right)^2 [1 - \Omega(k_\perp)] k_\perp^2/k_\parallel v_{te}\right] \partial n/\partial x \qquad (48)$$

and

$$Q_e = T_e \Gamma_e \quad , \qquad (49)$$

where $\Gamma_e = \pi n v_x$ and $Q_e = \pi n m v^2 v_x/2$. Using the fluctuation spectrum obtained in Sec. IV, we find $\Gamma_e = -D_e \partial n/\partial x$, with

$$D_e = \frac{2 \times 10^{-8} \exp\{2[(L_s/L_n)/(L_s/L_n)_c]^{5/3}\} (B/10\ \text{kG})^2}{(n/10^{14}\ \text{cm}^{-3})(T_e/1\ \text{keV})^{1/2}}\ \text{cm}^2/\text{sec} \quad . \qquad (50)$$

It follows from the conservation of momentum that the particle flux is ambipolar. Hence, $D_i = D_e$.

Equation (50) describes the anomalous transport associated with the collisionless drift mode in a hydrogen plasma with no temperature gradients, and a temperature ratio of $T_e/T_i = 4$. This result has been derived from a slab model and does not include effects such as ∇B drifts and trapped particles that may be important in more complicated geometries. It is interesting to note that this transport coefficient yields containment times proportional to $nT_e^{1/2}$, and that the diffusion coefficient increases (and the containment time decreases) rapidly with L_s/L_n.

VI. DISCUSSION

We have developed a formalism for studying the fluctuations of weakly damped normal modes in an inhomogeneous plasma. This formalism extends previous work[9] on the fluctuation spectrum in the absence of normal modes. It is used to evaluate the fluctuation spectrum of the collisionless drift wave in a sheared magnetic field. Both the coherence and the amplitude of the fluctuation spectrum are found to increase in the limit of weak magnetic shear. The fluctuation spectrum is used together with the quasilinear transport coefficients to evaluate the transport associated with the collisionless drift mode. The transport rates are found to be anomalously large in the limit of weak magnetic shear.

The range of validity of this calculation is restricted at both large and small values of L_s/L_n. In the limit of strong shear, $L_s/L_n \quad (L_s/L_n)_c = 20$, the WKB approximation introduced in Sec. II breaks down. Since the formalism of Sec. II remains valid in this limit, our calculation could be extended to include this strong shear limit. We have chosen not to do this because the scaling of $(e\phi/T)$ described by Eq. (47) indicates that the fluctuation level will be uninterestingly small in this limit.

Our expression for $\langle (e\phi/T_e)^2 \rangle$ grows without bound in the limit of weak magnetic shear. Clearly, our assumption of a linear plasma response, cf, Eq. (2), must break down in this limit. The nonlinear interaction of drift waves has been studied extensively.[1] Although this field is still an active area of current research, there seems to be a general concensus that nonlinear effects become important at amplitudes $\langle (e\phi/T_e)^2 \rangle \sim (\rho_s/L_n)^2$.

In addition to the mode-coupling and strong-turbulence theories discussed in Ref. 1, we note that the trapping of resonant electrons by the wave may be important due to the coherence of the fluctuation spectrum obtained in Sec. IV. Particle trapping[19] will occur at amplitudes $\langle(e\phi/T_e)^2\rangle \sim (9L_n\nu_e/v_{te})^{4/3}$. As either of these limits on $\langle(e\phi/T_e)^2\rangle$ is approached our assumption of a linear plasma response breaks down, and Eqs. (47) and (50) are no longer valid.

ACKNOWLEDGMENTS

We are pleased to acknowledge helpful conversations with Drs. Carl Oberman, William Tang, Roscoe White, and John Krommes. In addition, one of us (WMN) would like to thank the Aspen Center for Physics for their hospitality while much of this manuscript was written.

This work was supported by the United States Department of Energy Contract No. EY-76-C-02-3073.

REFERENCES

[1]See the review article by W.M. Tang, Nucl. Fusion 18, 1089 (1978).

[2]D.W. Ross and S.M. Mahajan, Phys. Rev. Letts. 40, 324 (1978).

[3]K.T. Tsang, P.J. Catto, J.C. Whitson, and T. Smith, Phys. Rev. Letts. 40, 327 (1978).

[4]Liu Chen, P.N. Guzdar, R.B. White, P.K. Kaw, and C. Oberman, Phys. Rev. Letts. 41, 649 (1978).

[5]T.M. Antonsen, Phys. Rev. Letts. 41, 33 (1978).

[6]Y.C. Lee and Liu Chen, Phys. Rev. Letts. 42, 708 (1979).

[7]Y.C. Lee, Liu Chen, and W.M. Nevins, Princeton Plasma Physics Laboratory Report PPPL-1544 (1979), to be published.

[8]N. Rostoker, Nucl. Fusion 1, 101 (1961).

[9]A. Kent and J.B. Taylor, Phys. Fluids 12, 209 (1969).

[10]D.E. Baldwin and J.D. Callen, Phys. Rev. Letts. 28, 1686 (1972).

[11]M. True, Ph.D. thesis, Princeton University (1977).

[12]P.M. Morse and H. Feshback, Methods of Theoretical Physics I (McGraw-Hill, New York, 1953).

[13]J. Heading, An Introduction to Phase Integral Methods, (John Wiley and Sons, New York, 1962).

[14]F.L. Hinton and M.N. Rosenbluth, Fusion Research Center, U. of Texas Report No. FRCR 197 (unpublished).

[15]See, e.g., J.N. Davidson and T. Kammash, Nucl. Fusion 8, 203 (1968).

[16]A similar result has been obtained independently by F.L. Hinton, M.N. Rosenbluth, op. cit.; and by T.M. Antonsen and S.M. Mahajan, Phys. Fluids 22, 1836 (1979).

[17]R. White, J. Comput. Phys. 31, 409 (1979).

[18]W. Horton, Phys. Fluids 19, 711 (1976).

[19]W.M. Nevins, Phys. Fluids 22, 1681 (1979).

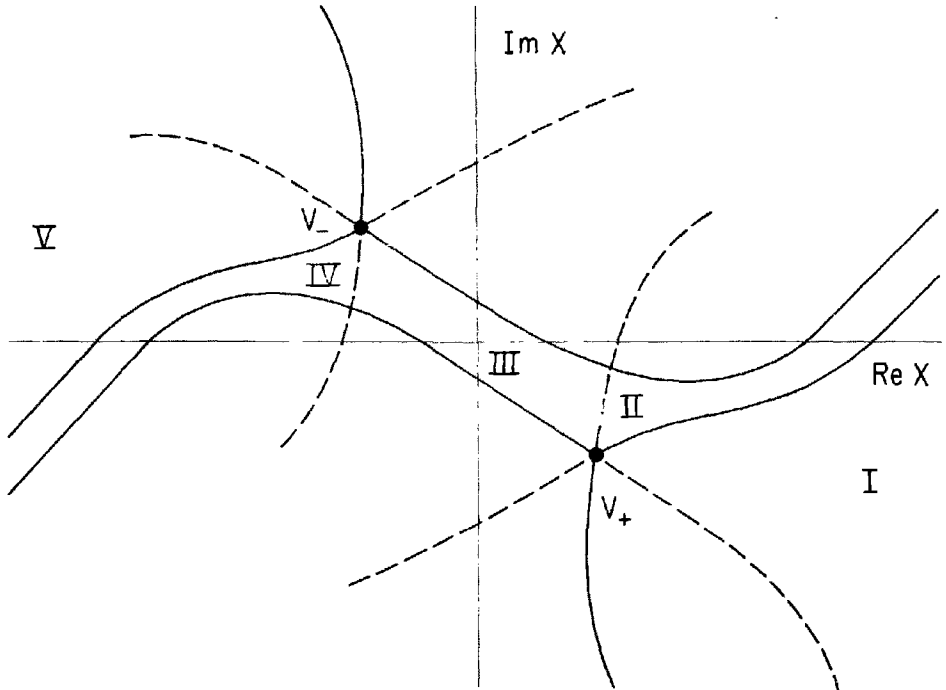

792409

Fig. 1. The Stokes structure at frequencies in the neighborhood of a normal mode frequency. The principle Stokes lines are dashed while the principle anti-Stokes lines are solid.

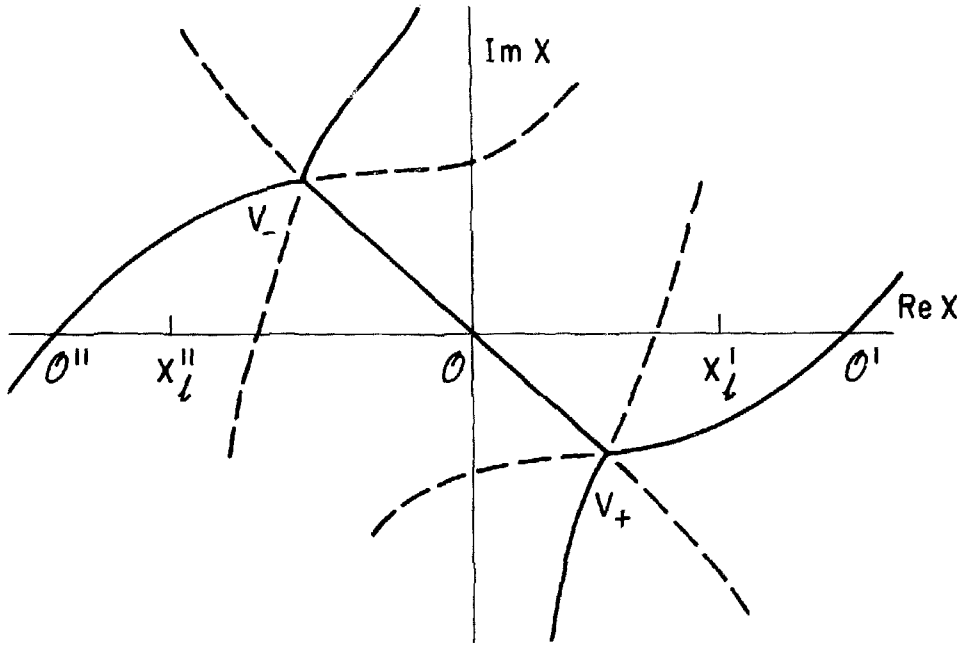

792411

Fig. 2. Stokes structure at a normal mode frequency in a convectively unstable plasma.

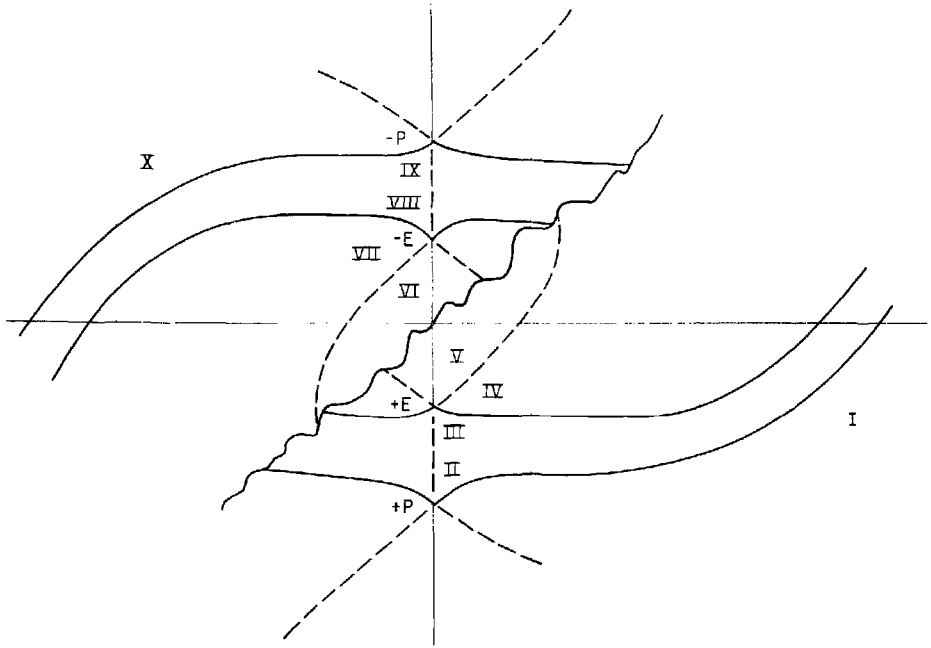

792415

Fig. 3. Stokes structure of the collisionless drift mode in the weak shear limit.

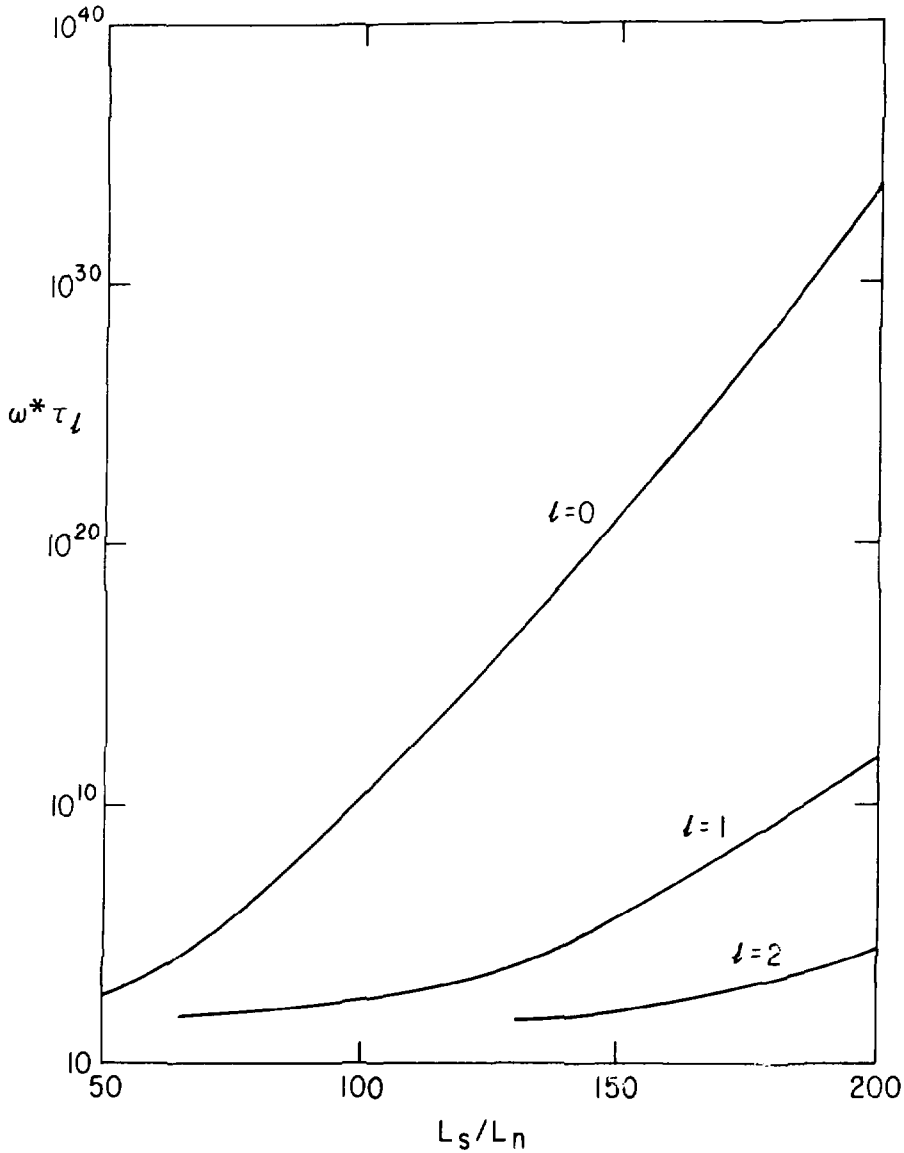

792417

Fig. 4. Decay time of modes $\ell \approx 0$ through $\ell \approx 2$ vs. L_s/L_n with b = 1, $T_e/T_i = 4$, and $m_e/m_i = 1/1837$.

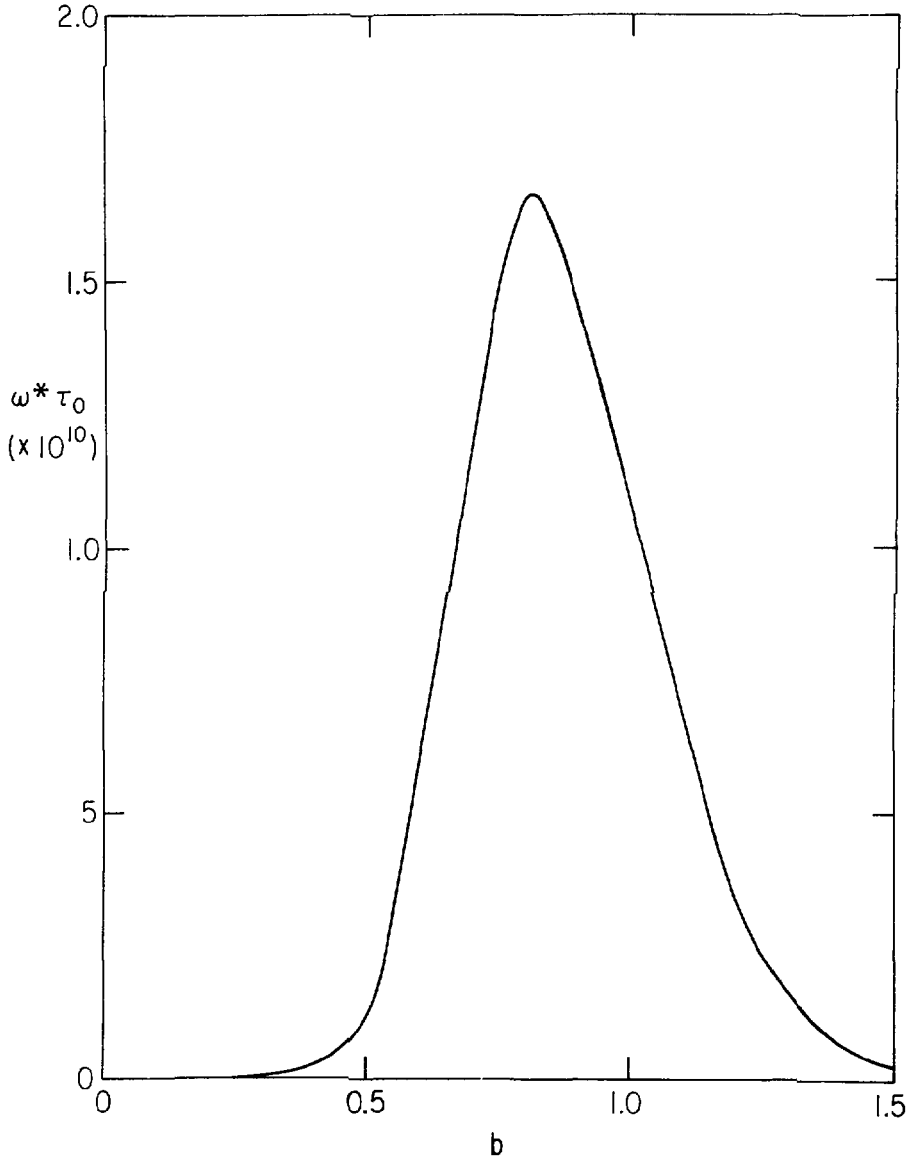

792410

Fig. 5. Decay time of $\ell = 0$ mode vs. b with $L_s/L_n = 100$, $T_e/T_i = 4$, and $m_e/m_i = 1/1837$.

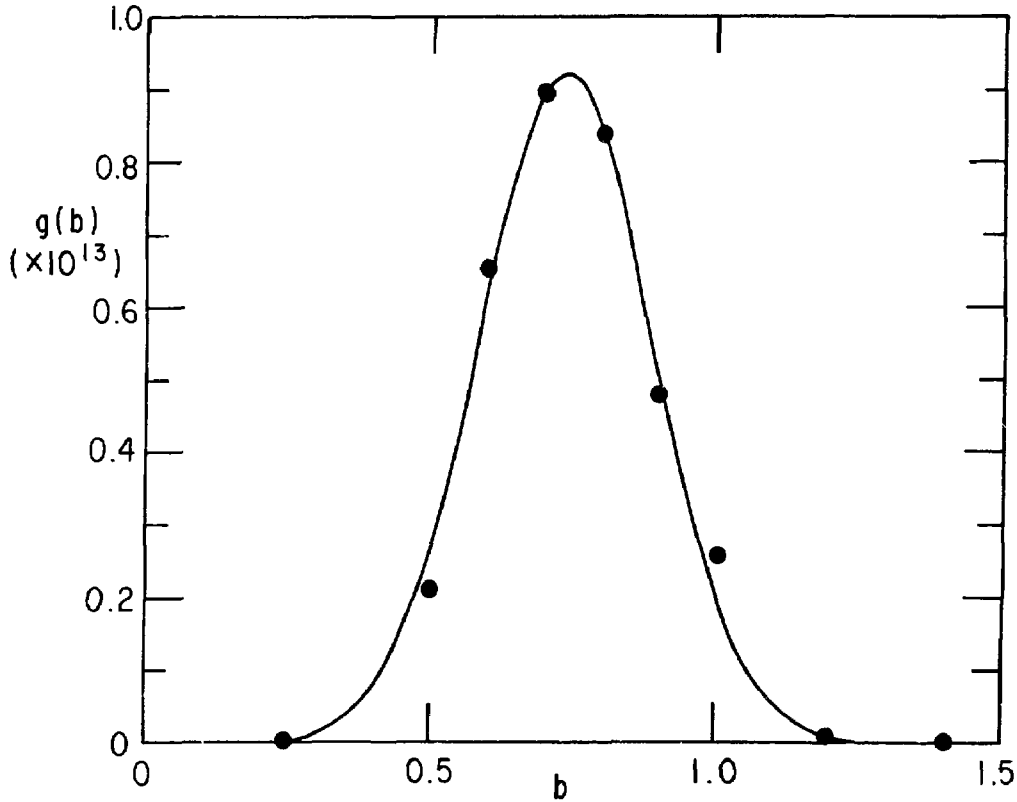

792548

Fig. 6. The normalized spectral density, g(b). Numerical values are indicated by dots, the Guassian obtained from a least squares fit is shown by the solid lines. $L_s/L_n = 100$, $T_e/T_i = 4$, $m_e/m_i = 1/1837$.

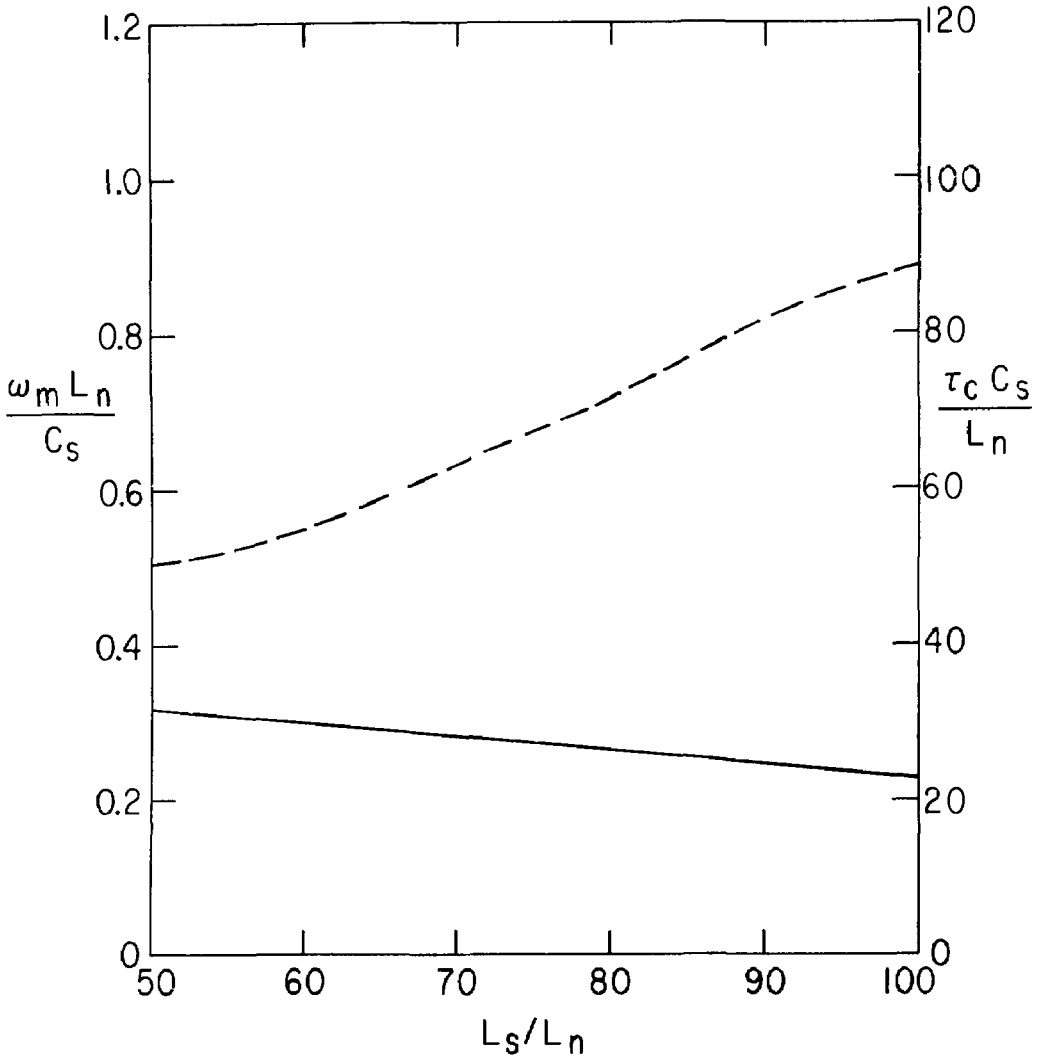

792554

Fig. 7. Mean frequency (solid line) and correlation time (dashed line) vs. L_s/L_n . $T_e/T_i = 4$ and $m_e/m_i = 1/1837$.

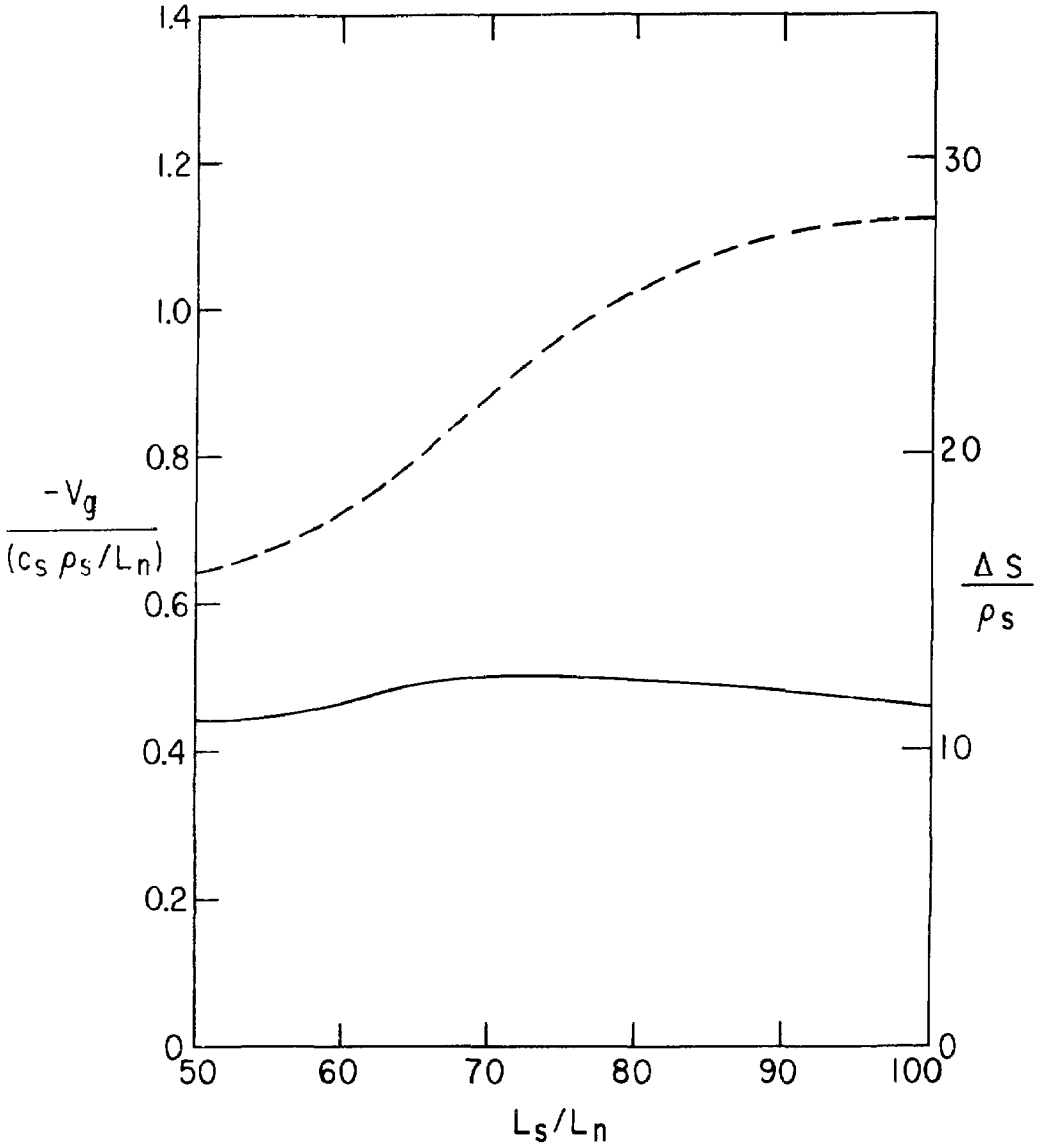

792565

Fig. 8. Group velocity (solid line) and phase mixing length (dashed line) vs. L_s/L_n.

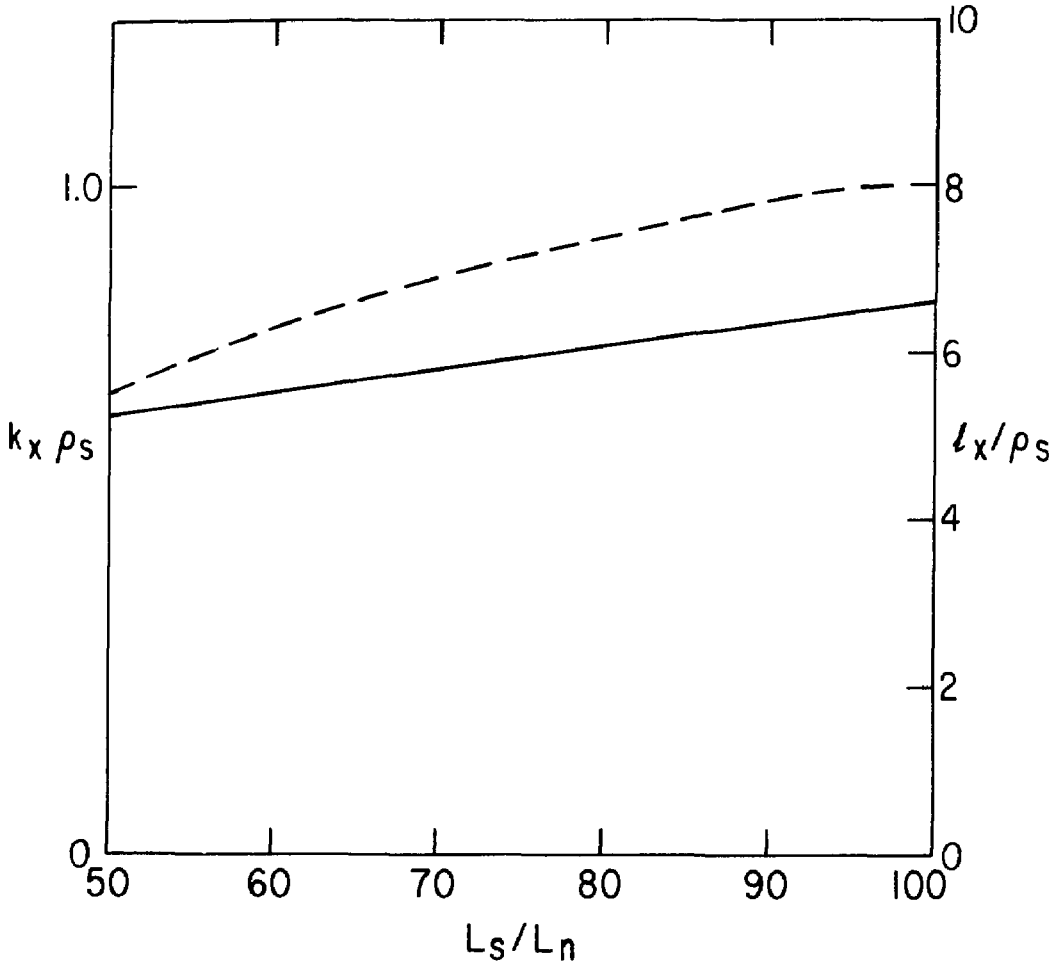

792553

Fig. 9. Mean wave number (solid line) and correlation length (dashed line) in the inhomogeneous (x) direction.

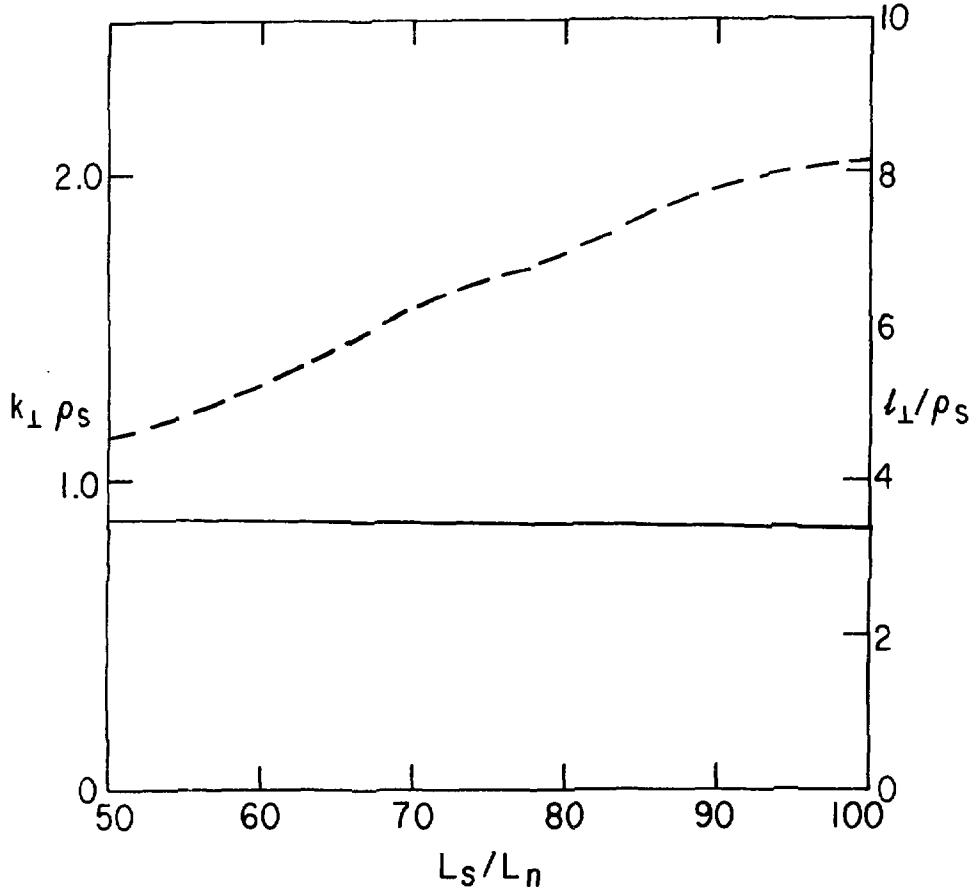

792550

Fig. 10. Mean wave number (solid line) and correlation length (dashed line) in direction perpendicular to both the magnetic field and the density gradient.

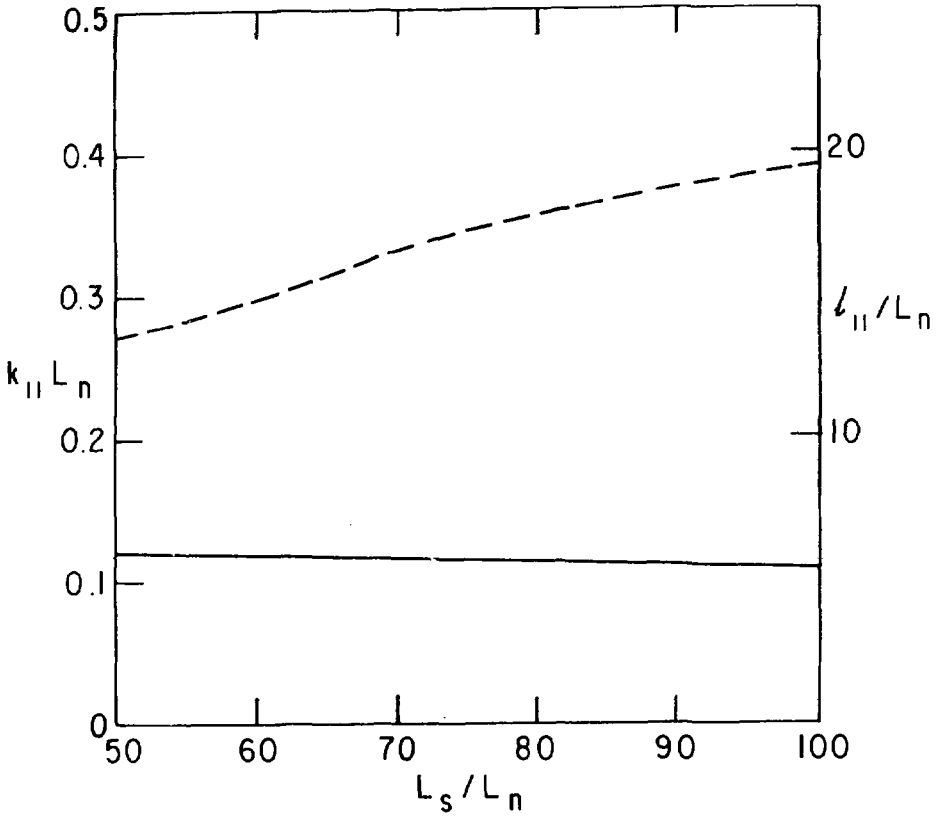

792549

Fig. 11. Mean wave number (solid line) and correlation length (dashed line) parallel to the magnetic field.

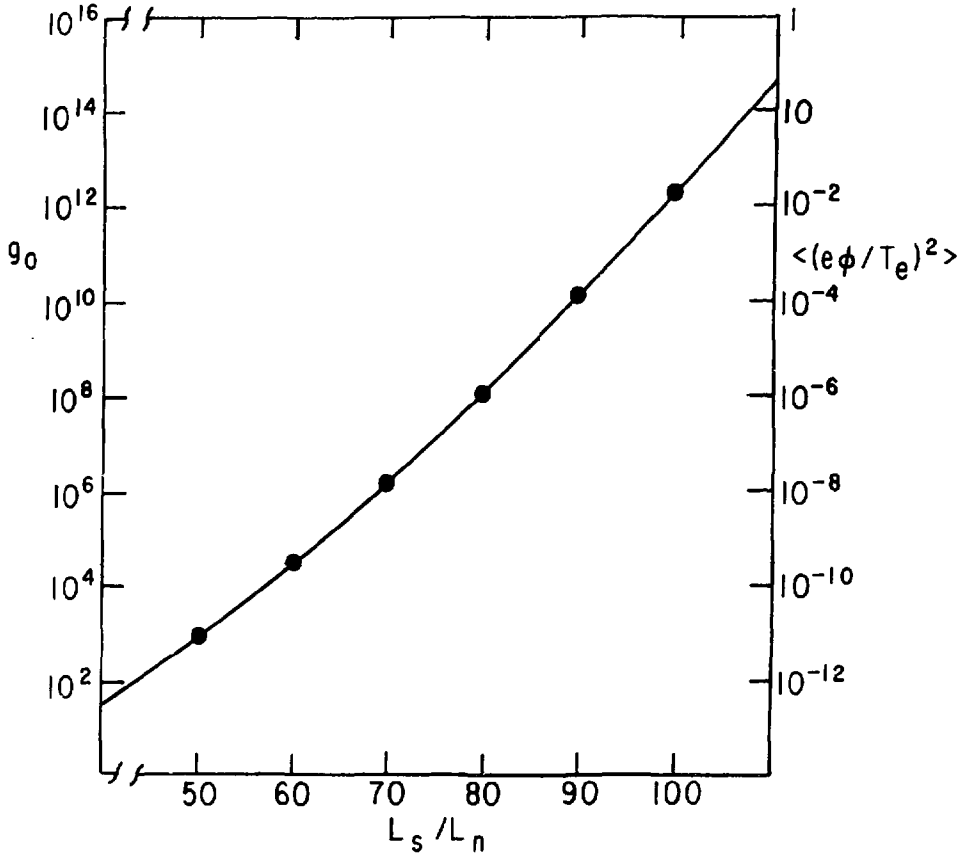

792552

Fig. 12. g_o (left scale) and $<(e\phi/T_e^2)>$ (right scale) for reference parameters $n = 10^{14}$ cm^{-3}, B = 10 kG, T_e = 1 keV, and L_n = 10 cm. Numerical values are indicated by dots, while the numerical approximation of Eq. (46) is shown as a solid line.